

Measurement of Aggregate Breakdown under Rain: Comparison with Tests of Water Stability and Relationships with Field Measurements of Infiltration

R. J. Loch and J. L. Foley

Queensland Department of Primary Industries,
P.O. Box 102, Toowoomba, Qld 4350.

Abstract

This paper reports comparisons between aggregate breakdown on wetting by rainfall with breakdown measured by a range of alternative methods. It also reports correlations between measured breakdown and steady infiltration rates of simulated rain of high and low energy, and hydraulic conductivities of surface seal layers formed under high energy rain. A wide range of soils in eastern Australia were studied.

Highly significant correlations were found between measurements of aggregate breakdown to $<125\ \mu\text{m}$ caused by rainfall wetting and both steady infiltration rates and hydraulic conductivities. Significant, but poorer correlations were found between steady infiltration rates and breakdown resulting from immersion wetting. Deletion of swelling soils from the data set greatly improved correlations between steady infiltration rates of high energy rain and breakdown measured by both immersion and tension wetting, showing that these methods of wetting are particularly inappropriate for swelling soils. No correlation was found between infiltration rates and measured clay dispersion.

Different relationships between the proportion of particles (%) $<125\ \mu\text{m}$ at the soil surface (P_{125}) and steady infiltration rates of low and high energy rain indicated that compaction of the soil surface layer, rather than increased aggregate breakdown, is a major cause of surface sealing by raindrop impacts. Measurements of fall cone penetration confirmed that drop impacts had compacted the surface layer.

Suctions across the surface seal were related to P_{125} in that layer, and the relationship obtained was used in calculating hydraulic conductivities.

The results confirm that measurement of aggregate breakdown under rainfall wetting produces results of much greater relevance to soil behaviour under field conditions than do tests based on immersion and tension wetting.

Introduction

A method for measuring and describing aggregate breakdown under rain has been proposed by Loch (1994). This paper compares results from the proposed rainfall wetting method with those from more commonly used tests of aggregate stability to wetting.

As well, this paper extends the appraisal of the proposed method to consider whether measured breakdown can be related to 'steady' infiltration rates of simulated rain into field plots, and to hydraulic conductivities of surface seal layers at that 'equilibrium' stage of surface seal development. The reason for focusing on steady infiltration rates is that size distributions in the surface seal layer tend to reach an equilibrium (Cleary *et al.* 1987; Loch *et al.* 1988) and, if

relationships of aggregate breakdown with field soil behaviour are being sought, then relationships between equilibrium size distributions and equilibrium (steady) infiltration rates are most likely.

Use of simulated rain was essential if the experimentation was to be practicable. When interpreting results of this study, and commenting on the field relevance of the various tests of aggregate breakdown, it is assumed that infiltration of simulated rain is consistent with that of natural rain of similar intensities and kinetic energies. There is evidence for this assumption, as Connolly *et al.* (1991) found that infiltration parameters derived from rainfall simulation studies gave good prediction of observed runoff hydrographs from field catchments.

In assessing whether the proposed measurement can be related to the infiltration behaviour of field soils, this paper addresses a major deficiency in information with respect to tests of aggregate stability in general (Loch 1994).

Methods

Stability/Breakdown Measurements

Size distributions of water-stable material (aggregates and primary particles) were measured by wet sieving after initially air-dry samples were wet by

- (i) immersion;
- (ii) -20 mm tension on filter papers placed on a tension table;
- (iii) high-energy rain for 20-30 min at 100 mm h^{-1} ;
- (iv) low-energy rain for 20-30 min at 100 mm h^{-1} ;

Dispersion ratios were also measured.

For rainfall wetting, the methods detailed by Loch (1994) were used, and all wet-sieving followed the methods proposed in that same paper.

Both high and low energy rain were used so that effects of rate of wetting could be separated from those of drop energy. Where samples for measurement of aggregate breakdown came from field plots, the durations of rain were greater than 20 min.

Immersion and tension wetting used 30 g samples of whole soil, wet in rainwater (conductivity $<0.03 \text{ dS m}^{-1}$) for 10 min and 24 h respectively, prior to wet-sieving. Immersion entailed samples being placed into 2 mm of water in a flat-bottomed dish.

Dispersion ratio measurements used 30 g samples of whole soil, ground to $<2 \text{ mm}$, immersed in 0.18 L of deionized water in bottles, and shaken in an oscillating shaker for 16 h. Dispersed clay was measured by pipette sampling, with the amount of clay dispersed by shaking expressed as both a percentage of the whole soil, or as a percentage of the clay in the soil.

Duplication of the tests was 8 for immersion and tension wetting, ≥ 8 for wetting by high and low energy rain, and 2 for dispersion ratios.

Soils

The study considered 23 soils, covering a wide range of particle size distributions and clay mineralogies (as indicated by cation exchange capacities) (Table 1) and locations (Fig. 1). Some of the soils were sampled from experimental areas where different tillage and/or fallow management practices were being compared and, for these soils, each tillage treatment was taken as a separate data point in comparing results of the various tests of aggregate breakdown.

Rainfall Simulation

All laboratory applications of simulated rainfall used a simulator based on a design by Bubenzer and Meyer (1965) with Veejet 80100 nozzles mounted on an oscillating manifold.

The simulated rainfall applications in the field used two different rainfall simulators, each with a different nozzle—the Veejet 80100 in a rainulator (Meyer and McCune 1958) and the 1 1/2 H30 in a rotating disc rainfall simulator (Morin *et al.* 1967). These nozzles were compared by Loch (1989) using a distrometer (Joss and Waldvogel 1967) to measure drop size,

and the Veejet 80100 had a slightly lower proportion of drops >2.25 mm diameter (Fig. 2). Due to the pulsing action of each rainfall simulator, the proportions of drops able to be counted by the distrometer were very low—12.6% for the 1 1/2 H30 nozzle in the rotating disc rainfall simulator at an intensity of 82.5 mm h^{-1} and 1.96% for the Veejet 80100 nozzle in a laboratory rainfall simulator at 100 mm h^{-1} intensity. (The bulk of the drops occurred

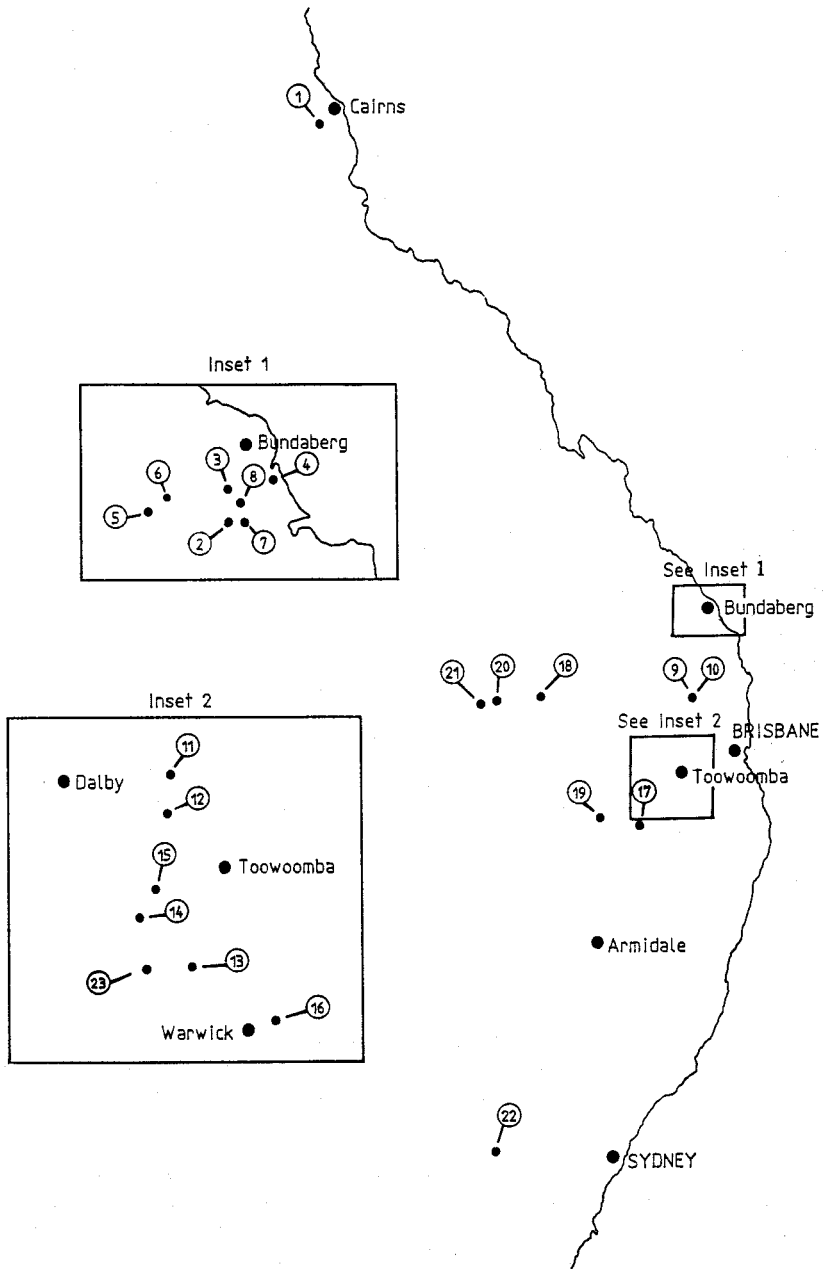


Fig. 1. Locations of the soils sampled in this study.

Table 1. Description of soils studied in comparing tests of aggregate stability

Soil No.	Great Soil Group	Soil Order	Particle size analysis				CEC (cmol/kg)
			% in sizes (μm) of				
			<2	2-20	20-200	>200	
1 ^A	krasnozem	Oxisol	62	13	16	9	18
2	yellow earth	Alfisol	13	2	78	6	5
3	lateritic podzolic	Alfisol	11	11	48	30	8
4	red podzolic	Alfisol	8	6	33	52	4
5	gleyed podzolic	Alfisol	12	21	46	21	6
6	yellow podzolic	Alfisol	14	9	52	25	8
7	soloth	Alfisol	9	18	68	5	2
8	gleyed podzolic	Ultisol	13	1	57	28	6
9	krasnozem	Alfisol	53	17	33	2	18
10	krasnozem	Alfisol	53	13	32	3	25
11	euchrozem	Inceptisol	43	12	38	7	20
12	grey clay	Vertisol	53	13	24	10	31
13	solodic	Alfisol	19	7	47	28	10
14	black earth	Vertisol	66	18	12	4	65
15	black earth	Vertisol	64	16	19	1	52
16 ^A	black earth	Vertisol	70	19	9	2	63
17	grey brown podzolic	Alfisol	19	32	46	3	10
18	red brown earth variant	Alfisol	25	5	62	8	20
19 ^A	red brown earth	Alfisol	24	16	55	6	16
20	brown clay	Vertisol	56	18	22	3	32
21	shallow podzolic	Alfisol	31	15	47	6	22
22 ^A	red brown earth	Alfisol	11	4	42	43	6
23	yellow podzolic	Alfisol	5	1	6	89	2

^A Soils on which experiments were being conducted to compare a range of tillage/fallow management strategies, see Table 2 for greater detail.

in bursts that could not be separated.) The 1 1/2 H30 nozzle has been reported to give a kinetic energy of $33.4 \text{ J m}^{-2} \text{ mm}^{-1}$ (Marston 1980). A range of estimates of kinetic energy have been given for the Veejet 80100, with possibly the most accurate assessment coming from Duncan (1972), who measured drop velocities directly and found that, with a fall height of 2.4 m, the smaller drops had velocities greater than the terminal velocities of similar-sized drops in still air, so that rainfall kinetic energy calculated for the Veejet 80100 nozzle on the basis of measured drop size and velocity was $29.49 \text{ J m}^{-2} \text{ mm}^{-1}$, very close to the kinetic energy in the order of $29 \text{ J m}^{-2} \text{ mm}^{-1}$ recommended by Loch (1994). Estimated kinetic energy of rain from the 80100 nozzle based on the distrometer measurements shown in Fig. 2 is $24 \text{ J m}^{-2} \text{ mm}^{-1}$ (Silburn and Foley, pers. comm.), but this can be expected to be a slight underestimate as the distrometer was only able to measure a low proportion of drops, mainly at the edge of the spray pattern where the drop size distribution is slightly finer (Duncan 1972).

It was concluded that either nozzle would give reasonable simulation of intense natural rain. Importantly, Loch (1989) found that both nozzles caused similar aggregate breakdown for three moderately stable soils (which are more responsive to drop energy than either unstable or highly stable soils).

To apply low energy rain, a layer of nylon mesh was suspended 100 mm above the soil surface to disrupt the raindrops. Distrometer measurements (Loch 1989) indicate that this procedure breaks all drops to less than 0.3 mm diameter and, hence, reduces kinetic energy to negligible levels. The mesh allowed reduction in drop energy without altering rainfall intensity or the pattern of rainfall application (as would be the case if different nozzles with different drop size distributions were incorporated into the rainfall simulators, both of which have an intermittent spraying action).

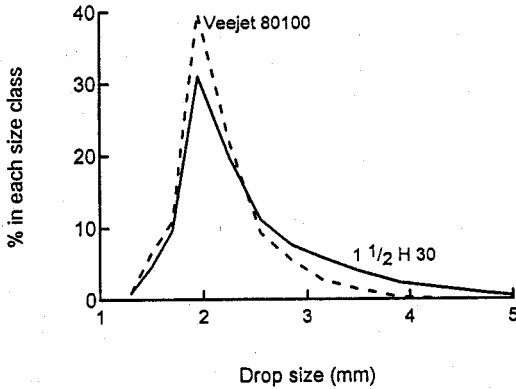


Fig. 2. Size distributions of drops measured for Veejet 80100 (dashed line) and 1 1/2 H30 (solid line) nozzles.

Table 2 lists the soils on which infiltration measurements were made, the rainfall simulator used, the rainfall energy used (high or low), and the number of replicates available for each soil or tillage treatment.

Table 2. Listing of soils studied, and rainfall simulators used in field infiltration studies

	Soil and tillage treatment ^A	Rainfall simulator ^B	No. of replicates of rain of	
			High energy	Low energy
1.	DD+S	RDS	2	2
	DD-S	RDS	3	3
	CT+S	RDS	3	2
	CT-S	RDS	2	2
2.		RDS	2	2
3		RDS	2	2
4		RDS	2	2
6		RDS	1	2
7		RDS	2	2
11.		rainulator	3	0
12.		rainulator	2	0
13.		rainulator	2	0
14.		rainulator	4	0
15.		RDS	3	3
16.	DD+S	RDS	3	3
	CT+S	RDS	3	3
17.		RDS	3	3
19.	RT+S	RDS	3	3
	RT-S	RDS	3	3
	CT+S	RDS	3	3
	CT-S	RDS	3	3
22.	DD+S	RDS	2	0
	RT+S	RDS	2	0
23.		RDS	2 ^C	2 ^C

^A Soils are numbered as in Table 1. DD, direct drill; RT, reduced tillage; CT, conventional (frequent) tillage; S refers to crop residues (stubble) either retained during fallow (+) or removed (-).

^B RDS, rotating disc rainfall simulator.

^C Number of rainfall simulator plots from which cores were taken for permeability measurements.

The methods used were subject to slight variations from site to site, and were:

- (a) Simulated rainfall of high or low energy was applied to field plots by the rainulator and rotating disc rainfall simulator (RDS). Intensities ranged from 50 to 100 mm h⁻¹, and rain was applied until a 'steady' infiltration rate was obtained. A 'steady' infiltration rate was defined as one that showed no change over three consecutive samplings of runoff rate. As runoff rate was measured at 3 min intervals, this is effectively a steady runoff rate over a 9 min period.
- (b) Rainulator plots were 12 m², RDS plots were 1 m².
- (c) Soils/tillage treatments used in this study were bare of stubble for the measurements of infiltration, even treatments that involved stubble retention during the fallow period between one crop and the next. This was done so that the measurements of infiltration reflected differences in size distributions of water-stable material at the soil surface, rather than differences in surface protection by crop residues. All soils and tillage treatments were freshly tilled or had some surface disturbance.
- (d) For all soils except soil 17, the rainfall simulator studies used field plots, and were carried out at times when the surface 100–200 mm of soil was close to air dry. For soil 17, plots of air-dried soil 1 m² in area and 150 mm deep overlying approximately 0.7 m of coarse sand were prepared and simulated rain was applied by means of the RDS. This was done because prolonged wet weather made field rainfall simulation on reasonably dry soil impossible. The use of a 150 mm deep plot of soil should not have affected the results obtained, as soil 17 rapidly formed a surface seal of particularly low permeability, with depths of wetting of 20 and 33 mm under rain of high and low energy respectively.
- (e) Rainwater (with electrical conductivity <0.03 dS m⁻¹) was used in all rainfall simulation.
- (f) For soil 23, which has a deep A horizon of coarse sand, permeability was too high for rainfall simulation to give a direct measure of infiltration. Instead, hydraulic conductivities were measured using the technique of Talsma (1969). Plots were exposed to rain at 70 mm h⁻¹ of high and low energy for 20 min, and then cores 300 mm diameter and 200 mm deep were taken. Water was ponded on the surface of the cores by using a constant head permeameter to measure hydraulic conductivity. Six cores were taken for each rainfall energy. The hydraulic conductivities are equated with steady infiltration rates [e.g. with the *A* term of the Philip (1957) equation as suggested by Williams and Bonell (1988)]. The 'infiltration rates' measured were considerably higher than those measured on the soils, and indicate the magnitudes of infiltration rate that can be expected at very low proportions of particles <125 µm.

Soil Sampling

Soil samples were taken adjacent to the rainfall simulator plots at the time of the experiments for subsequent laboratory measurements of aggregate breakdown under rain. The only exceptions were soils 11 and 12, for which samples were taken some time after the infiltration studies.

Samples were taken from the tilled (and mixed) layer of tilled soils (typically 0–100 mm depth), and from the 0–20 mm layer of direct-drilled soils (and of all treatments on soil 1, which was not tilled, but only raked to destroy macropores). All samples were air-dried, and stored in air-tight containers.

Methods for Describing Size Distributions/Degrees of Breakdown

A range of methods for describing size distributions were tested, including larger groupings of size classes and mean weight diameter (MWD; Chaney and Swift 1984) and geometric mean diameter (GMD; Mazurak 1949). The MWD was calculated as:

$$\text{MWD} = \sum (F_n D_n), \quad (1)$$

where F_n is the proportion of sample in size class n , and D_n is the mean diameter of size class n .

The GMD was calculated as

$$\text{GMD} = \text{antilog}\left\{\frac{\sum(W_n \log D_n)}{\sum W_n}\right\}, \quad (2)$$

where W_n is the weight of material in each size class.

Surface Soil Strength

Within 15 min of rainfall ceasing, a fall-cone penetrometer (80 g cone, 30° cone angle) was used to assess the shear strength of the soil surface after exposure to rain of high or low energy. Measurements were made during both laboratory and field studies on most of the soils shown in Table 1. [Fall-cone measurements have been widely used to assess development of compaction and cohesion under rainfall (Al-Durrah and Bradford 1982; Schultz *et al.* 1985; Bradford *et al.* 1987a, 1987b; Nearing and West 1988).]

Measurement of Seal and Subseal Properties for Calculation of Seal Hydraulic Conductivity

For any given layer of soil, Darcy's Law gives the flux (i) of water through it as

$$i = K \Delta H/L, \quad (3)$$

where K is the hydraulic conductivity, and $\Delta H/L$ is the hydraulic head gradient across the layer of thickness L . For a surface seal, $\Delta H/L$ can be expanded to $(H_o - H_c + L_c)/L_c$, where H_o is the hydraulic head at the seal surface, H_c is the hydraulic head at the bottom of the seal, and L_c is the thickness of the seal. It is common to assume the depth of ponded water on the seal to be negligible, and therefore $H_o = 0$, so that equation (3) can be rearranged to

$$K = iL_c/(L_c - H_c). \quad (4)$$

Therefore, derivation of K requires measurement of i , H_c and L_c . Measurement of i is described in preceding Sections. Surface seal thickness (L_c) was estimated visually.

For surface seals developed under high energy rain, H_c and L_c were determined for a limited number of the soils listed in Table 1. The soils were selected to cover the range in aggregate stability that was observed.

Matric potential below the surface seals (H_c) was measured by the following two methods.

Gravimetric samples. These were taken from a layer several mm thick below the surface seals, and potential was estimated from matric potential/gravimetric water content relationships for these soils, based on samples wet under tension—the method of wetting most likely to have occurred in the subseal layer. To avoid problems of low bulk density (and large quantities of inter-aggregate water at low suctions), moisture characteristic curves were determined on 5–2 mm aggregates, with the sample being sufficiently small for aggregate contact (and volume of inter-aggregate pores) to be minimal. Samples of the subseal layer were taken for measurement of water contents within 4 min of rain ceasing, as changes in gravimetric water content of the subseal layer were small during that period. In some cases, this approach could be applied with confidence, as the water contents intercepted the part of the matric potential/water content curve where matric potential was relatively insensitive to water content. However, for other soils, water contents intercepted the part of the curve where matric potential was highly sensitive to water content and, hence, matric potential was derived with less precision.

Disc permeameters (Perroux and White 1988). These were used to estimate the hydraulic potential across surface seals. The concept applied was that water would move into the soil only if the suction across the seal was greater than that at which water was held by the disc permeameter.

Disc permeameters set at a range of tensions were placed directly on the soil surface immediately rainfall ceased, and observed for the presence/absence of water movement. The tensions used and the intervals between tensions were varied depending on the soil, but commonly tensions in the range 40–90 mm were used, with intervals of 10–25 mm. The rate

of water movement into the soil could not be used to calculate K , as the method of placement of the permeameter on the soil surface did not give complete contact with the soil surface.

Results and Discussion

Comparison of Methods for Describing Water-Stable Size Distributions

To assess relationships between the various methods of describing size distributions and breakdown, Table 3 shows correlations between the proportions of water-stable material (aggregates and ultimate particles) <500 , <250 and $<125 \mu\text{m}$, together with MWD and GMD for samples of the soil surface exposed to high energy rain.

Table 3. Correlation matrix showing value and significance of correlation coefficients (r)* for various size parameters for 34 soils (or tillage treatments) wet by high energy rain

* $P < 0.001$ for all r values

Parameter	1.	2.	3.	4.	5.
1. % $<125 \mu\text{m}$	1.00				
2. % $<250 \mu\text{m}$	0.78	1.00			
3. % $<500 \mu\text{m}$	0.70	0.93	1.00		
4. MWD (mm)	-0.61	-0.76	-0.90	1.00	
5. GMD (mm)	-0.65	-0.81	-0.91	0.95	1.00

The larger the size class, the stronger its negative correlation with GMD and MWD (Table 3). The GMD and MWD are strongly correlated (Table 3), indicating little difference between these two indices of aggregate size for this data set. Also, both indices perform worse than percentages <250 and $<500 \mu\text{m}$ as indicators of the proportion of particles $<125 \mu\text{m}$ (as %, and referred to as P_{125}).

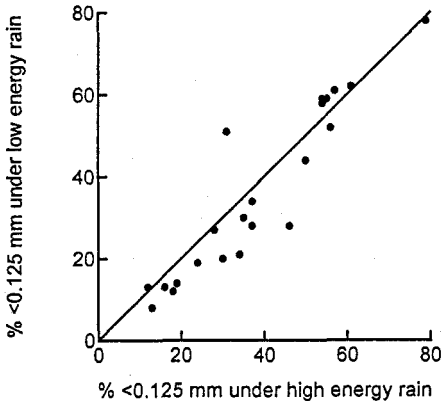


Fig. 3. Comparison of proportions of particles $<125 \mu\text{m}$ after wetting by simulated rain of high and low energy, 1:1 line shown.

Comparison of Results from the Tests Studied

Within the wet-sieving tests, both energies of rainfall wetting and immersion gave similar mean values of P_{125} (36.0, 38.5 and 36.1 for low energy rain, high energy rain, and immersion wetting respectively). Wetting under tension gave a mean P_{125} of only 17.3%.

Rainfall wetting

Wetting by low-energy rain gave results that explained 87% of the variation in the results from wetting by high energy rain (based on P_{125}), with the two rainfall wetting methods giving the closest agreement of any of the wetting methods compared. One sample (a tillage treatment on soil 16) gave much higher breakdown to $<125 \mu\text{m}$ under low energy rain (Fig. 3), and no explanation for this result is apparent. Breakdown to $<125 \mu\text{m}$ was generally slightly less under low energy rain than for high energy rain for the 'moderately stable soils' and little affected by drop energy for the stable and highly unstable soils, as shown in Fig. 3. Nonetheless, the effects of drop energy on breakdown to $<125 \mu\text{m}$ were generally small (Fig. 3), and it appears that the major reason that high and low energy rain caused similar amounts of aggregate breakdown is that they involve similar wetting rates. This suggests that, for most soils, wetting rate is of greater importance than drop impact as a factor in aggregate breakdown on wetting. Therefore, accurate simulation of rainfall kinetic energy may not be of critical importance in defining a test to suit field conditions.

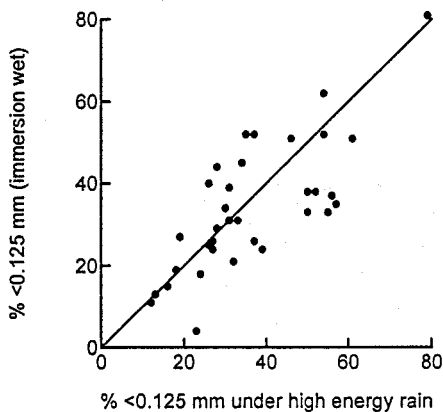


Fig. 4. Comparison of proportions of particles $<125 \mu\text{m}$ after wetting by simulated rain of high energy and by immersion, 1:1 line shown.

Immersion Wetting

Although immersion wetting caused similar breakdown to $<125 \mu\text{m}$ on average to that from rainfall wetting, results from immersion wetting explained only 40 and 49% of the variation in P_{125} measured by wetting with rain of low and high energy respectively. This is illustrated in Fig. 4 by the spread of data points about the 1:1 line for the comparison of immersion and high energy rain wet samples. The fact that immersion wetting gave greater breakdown than rainfall wetting at 100 mm h^{-1} for a number of soils indicates that, unlike the results of Coughlan (1979), wetting at 100 mm h^{-1} did not cause maximum aggregate breakdown but, for those soils, the even higher wetting rates associated with immersion wetting caused even greater breakdown. This apparent response to wetting rates $>100 \text{ mm h}^{-1}$ may only apply when wetting rates are greatly in excess of 100 mm h^{-1} , but in future studies there may be value in assessing whether wetting rates affect aggregate breakdown within the range of likely rainfall rates, e.g. from 50 to 100 mm h^{-1} .

For one of the two soils where immersion wetting gave lower breakdown than low energy rain, samples from four different tillage managements all showed

the same response, and the extra length of time available for wetting when rainfall wet may have allowed the aggregates to wet more fully and break down more completely. The soil (soil 19) tends to be hard setting, and slow and incomplete wetting (as noted by Brewer and Blackmore 1956) could explain its apparent stability to immersion wetting.

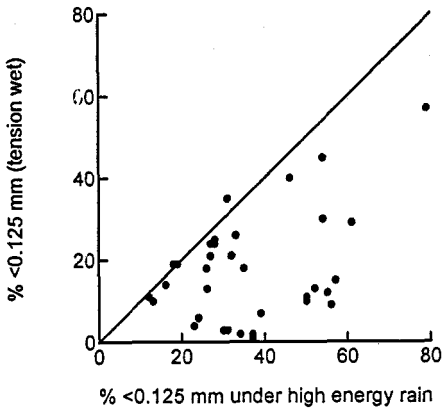


Fig. 5. Comparison of proportions of particles $<125 \mu\text{m}$ after wetting by simulated rain of high energy and by tension, 1:1 line shown.

Tension wetting

Tension wetting gave the weakest correlations with the other wet-sieving based tests. The relatively low breakdown to $<125 \mu\text{m}$ caused by tension wetting is shown clearly by its comparison with results of wetting by high energy rain (Fig. 5), with most of the data points below the 1:1 line. Proportions $<125 \mu\text{m}$ after tension wetting correlated most strongly with those resulting from immersion wetting, and least strongly with wetting by low energy rain (taking into account differences in numbers of samples).

Dispersion ratios

There was no significant correlation between wet-sieving and dispersion ratio approaches.

Overview

The results illustrate that a range of mechanisms control aggregate breakdown on wetting, and that these mechanisms interact with the wetting method. Rainfall wetting gives results considerably different from those of immersion, and is an essential component of tests for soils for which rainfall is the major or sole cause of wetting under field conditions.

Relationships between Steady Infiltration Rates under High Energy Rain and Aggregate Breakdown

Figs 6 and 7 show significant relationships between steady infiltration rates of high energy rain and some measurements of sizes of particles (aggregates and primary particles) under different wetting regimes. There is a highly significant relationship ($P < 0.001$) with the P_{125} measured after wetting by high energy rain (Fig. 6a). Data for the coarse sand were not used in Fig. 6a, because of difficulties of scale.

The relationship shown in Fig. 6a is likely to be broadly applicable, both because of its strength and because it was derived for a wide range of soils in terms of soil properties, geographic location and parent materials. It provides clear evidence of the value of the method for measuring size distributions of water-stable material at the soil surface under rain. The relationship is most variable for soils with low proportions $<125 \mu\text{m}$. This is possibly because some of the larger aggregate size fractions may have had greater effects on infiltration rates when pores were larger and the proportion of fine particles was low, and may also be due to increasing effects of the depth of wetted soil on infiltration rates for the more permeable soils.

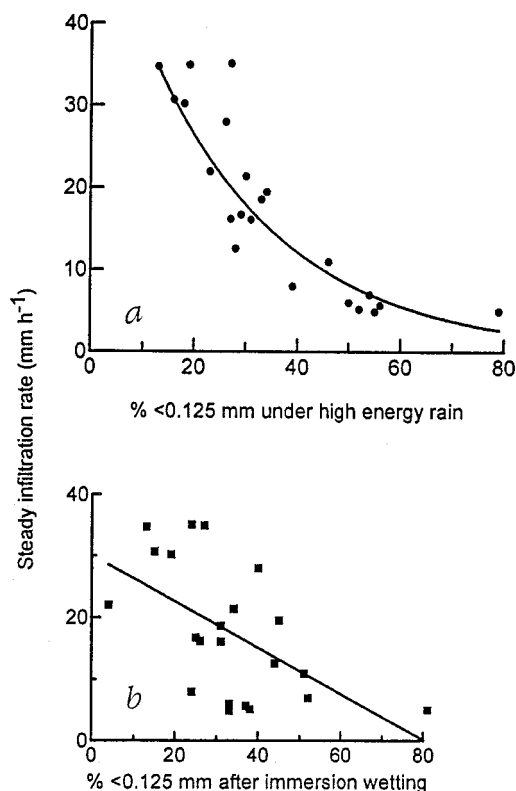


Fig. 6. Relationships between steady infiltration rates of high energy simulated rain and P_{125} (a) at the soil surface under high energy rain, $Y = 57.42e^{-0.0389X}$, $R^2 = 0.83$, and (b) after immersion wetting, $Y = 30.1 - 0.374X$, $R^2 = 0.32$.

The shape of the curve shown in Fig. 6a is consistent with what would be expected: an initial sharp decrease in hydraulic conductivity as P_{125} increased and coarse pores were blocked, with the data showing little further decrease in infiltration rates once P_{125} reached values $>50\%$, at and above which a fine matrix (and finer pore sizes) would be dominant in the surface seal. Although a fine matrix could be expected to develop at $>35\%$ $<125 \mu\text{m}$ in an ideal ternary mixture, the P_{125} needed for minimum void ratio would be increased if coarse particles were not thoroughly compacted (because the presence of finer particles prevented compaction of the coarse size class). Evidence of such 'dilation' of coarse particles was reported by Smith *et al.* (1978), who found the transition from coarse to fine matrix occurring at approximately 50% fine material.

In comparison with the data for rainfall wetting, there was statistically significant ($P < 0.01$) but relatively poor correlation of steady infiltration rates with the P_{125} after immersion wetting (Fig. 6*b*), and no correlation between steady infiltration rates and both the P_{125} measured after tension wetting and measured dispersion.

For rainfall-wet surfaces, the size fraction used as an indicator of breakdown under high energy rain affected the shape of the relationships obtained, but larger size fractions (Figs 7*a* and 7*b*), mean weight diameter (MWD) (Fig. 7*c*) and geometric mean diameter (not shown) also showed significant and strong relationships with steady infiltration rates of high energy rain. The strong correlations between particles <250 and $<500 \mu\text{m}$ and steady infiltration rates (Figs 7*a* and 7*b*) were to be expected, as these two size fractions and P_{125} are strongly correlated (Table 3). This illustrates that the selection of a size fraction to correlate with steady infiltration rate is not necessarily a crucial decision.

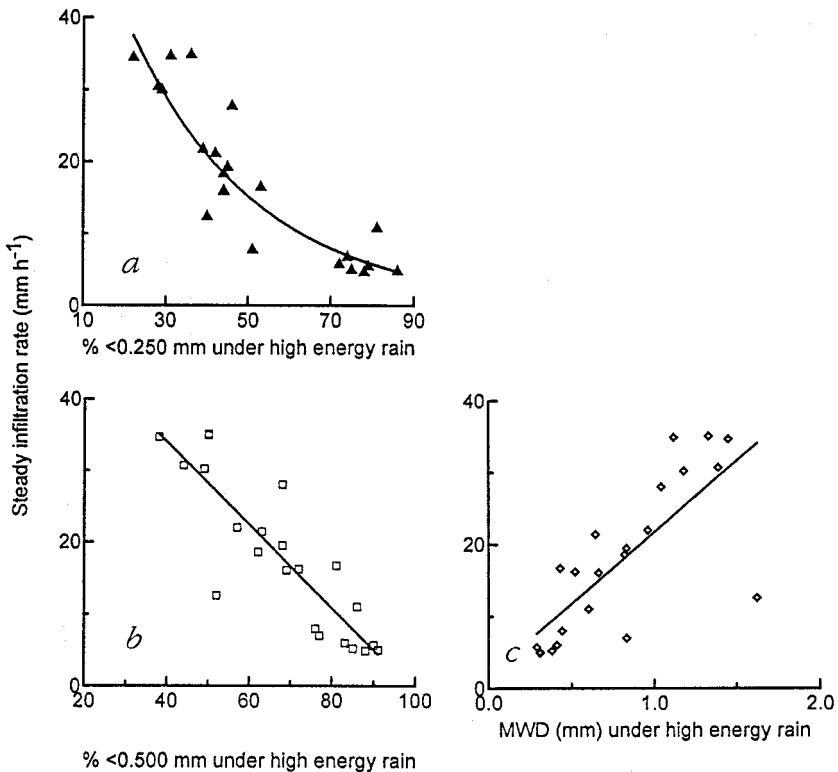


Fig. 7. Relationships between steady infiltration rates of high energy rain and (a) % $< 250 \mu\text{m}$ at the surface under rain, $Y = 76.39e^{-0.0323X}$, $R^2 = 0.83$, (b) % $< 500 \mu\text{m}$ at the surface under rain, $Y = 52.16 - 0.579X$, $R^2 = 0.77$, and (c) MWD of particles at the surface under rain, $Y = 1.85 + 19.862X$, $R^2 = 0.58$.

Steady Infiltration Rates for Low Percentages $<125 \mu\text{m}$ —Data for Soil 23

Soil 23 extends the data to an extremely low P_{125} . Conductivities were extremely high, 870 and 1170 mm h^{-1} for cores exposed to high and low energy

rain respectively. Hydraulic conductivity was significantly higher ($P < 0.05$) under low energy rain. The P_{125} in the surface layers was very low, being 5.0 and 5.6% in the 0-3 and 3-6 mm layers respectively of the rain-impacted surface, and 2.7 and 4.1% in the corresponding layers under low energy rain. The 3-6 mm layer was sampled because the surface layer did not appear to be compacted nor to be a throttle to infiltration under high energy rain.

The data for this soil show clearly that use of MWD and GMD is not likely to give useful correlations with infiltration rates. Unlike P_{125} , neither of these parameters showed soil 23 to be different from the other soils studied, and did not indicate the large differences in steady infiltration rates observed. The MWD and GMD were 0.73 and 0.91 mm respectively for soil 23, and can be compared with the values for MWD of the soils shown in Fig. 7c. This is further evidence that it is the fine size classes such as that $<125 \mu\text{m}$ that affect infiltration rates and surface seal development, rather than the coarser size classes (which largely determine values of MWD and GMD).

It appears that raindrop impact reduces hydraulic conductivity of the surface layer, even for soils of extremely high hydraulic conductivity.

Effects of Soil Swelling on Measurement of Breakdown by Immersion and Tension Wetting

Proportions $<125 \mu\text{m}$ after immersion and tension wetting were relatively poorly related to steady infiltration rates of high energy rain. However, when all the soils observed to crack on drying under field conditions were excluded, steady infiltration rates were significantly related ($P < 0.01$ and <0.001 respectively) to P_{125} after tension and immersion wetting (Figs 8a and 8b). Further, if the proportions $<125 \mu\text{m}$ for the 'non-swelling' soils are compared across wetting treatments, the results from both tension and immersion wetting correlate strongly with those after rainfall wetting (R^2 values of 0.88 and 0.87 respectively, $P < 0.001$ for both).

The improved correlation when swelling soils are excluded shows that a major problem with tests using immersion or tension wetting is their application to swelling clay soils, which are highly sensitive to wetting rate (Coughlan 1979, 1984). However, even with swelling soils excluded, the correlation between tension and immersion wetting results and steady infiltration rates is poor relative to that obtained from rainfall wetting.

Relationships between Steady Infiltration Rates of Low Energy Rain and Aggregate Breakdown

There was an extremely strong relationship ($P < 0.001$) between P_{125} and steady infiltration rate (both for low energy rain) (Fig. 9a). There was no significant correlation between steady infiltration rates and the P_{125} after tension wetting, but significant ($P < 0.01$) correlation with the P_{125} after immersion wetting (Fig. 9b).

The relationship between P_{125} at the soil surface and steady infiltration rates of low energy rain is similar in form to that obtained for high energy rain. No doubt a response to pore size is involved in both instances. Other approaches to the estimation of conductivity from particle size have considered the presence of

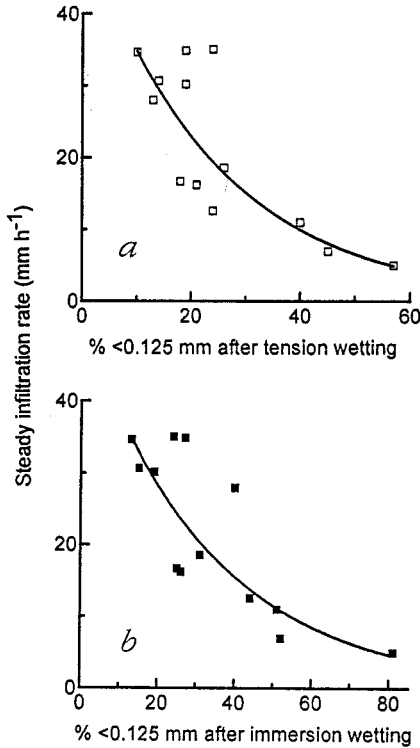


Fig. 8. Relationships for non-swelling soils only between steady infiltration rates of high energy rain, and (a) P_{125} after tension wetting, $Y = 52.82 e^{-0.0416X}$, $R^2 = 0.79$, and (b) P_{125} after immersion wetting, $Y = 51.48 e^{-0.0299X}$, $R^2 = 0.77$.

fine particles in more or less direct fashions. For example, the Carman (1956) equation relates conductivity to porosity and particle surface area. Mason *et al.* (1957) found hydraulic conductivity negatively correlated with soil silt and clay content, and only poorly correlated with bulk density (further evidence of the importance of pore sizes). Horn (1971) attempted to relate hydraulic conductivity to a combination of texture, structure, and clay dispersibility. Boon and Savat (1980) presented a nomogram relating soil permeability to median grain size and clay content.

Relative Importance of Drop Impacts and Aggregate Breakdown to Steady Infiltration Rates of Rain

Comparison of the curves for steady infiltration rates of high and low energy rain against P_{125} at the soil surface (after wetting by rainfall of high or low energy) (Fig. 10) shows that drop impact causes a reduction in steady infiltration rates over and above any effects of drop impact on aggregate breakdown and, hence, on P_{125} at the surface.

The reduction in infiltration rates due to drop impact is attributed to compaction of the soil surface, which would cause a general reduction in pore sizes. As evidence of compaction, fall-cone measurements showed significantly ($P < 0.01$) lower fall-cone penetration into raindrop impacted soil, indicating significant consolidation of the surface layer by raindrops. By assuming all other factors to be equal, increased soil shear strength can be attributed to increased soil bulk density (Cruse and Larson 1977).

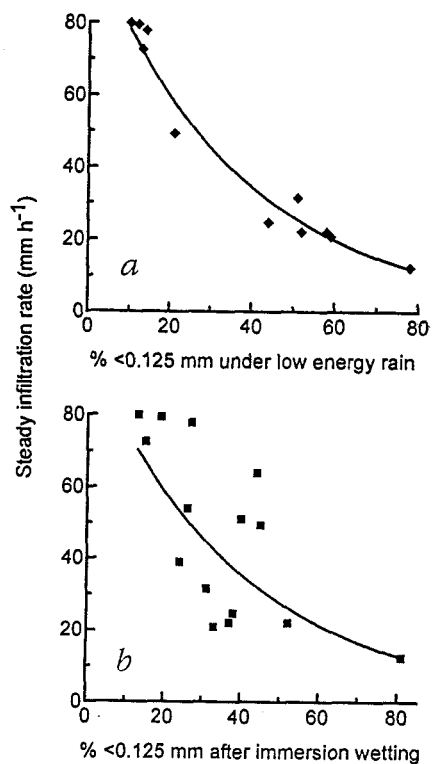


Fig. 9. Relationships between steady infiltration rates of low energy rain and (a) P_{125} at the soil surface under low energy rain, $Y = 103.15 e^{-0.0274X}$, $R^2 = 0.97$, and (b) P_{125} after immersion wetting, $Y = 97.68 e^{-0.0253X}$, $R^2 = 0.52$.

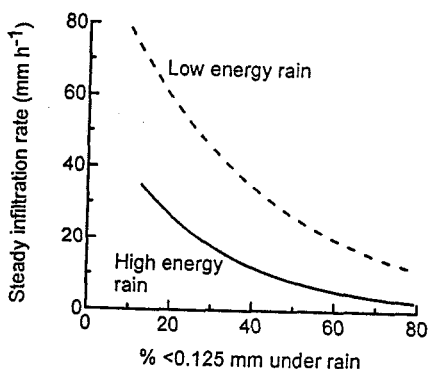


Fig. 10. Relationships between steady infiltration rates of rain of high and low energy and P_{125} at the soil surface under these rainfall energies.

Raindrop impact is widely reported as a major factor in surface seal development (Duley 1939; McIntyre 1958; Epstein and Grant 1973; Norton 1987), and it is generally suggested that raindrops cause surface sealing by increasing aggregate breakdown. However, results in Fig. 3 show that drop impact did not greatly increase aggregate breakdown for many soils. Therefore, it can be concluded that compaction of the surface layer by raindrops is the major mechanism by which raindrop impact causes surface sealing.

Use of different rainfall simulators (with different rainfall kinetic energies) could be expected to mainly affect the degree of compaction of the soil surface. Hence,

use of a range of drop kinetic energies could produce a series of relationships between steady infiltration rates and P_{125} , with the two curves shown in Fig. 10 being an indication of the likely range of relationships that would be obtained.

For virgin soils and one direct drilled soil, the presence of considerable partially decomposed organic material in the surface layer appeared to greatly reduce compaction of the surface layer, even when the soil was bare of cover.

Properties of Surface Seals

The thicknesses measured were quite consistent, with surface seal thicknesses ranging from 2.5 to 3.5 mm—probably because all soils studied were in a relatively fine tilth. The data agree well with previously published data showing seal thicknesses to be typically close to 3 mm, and an average seal thickness of 3 mm was adopted in calculations of hydraulic conductivity. (For soils or situations where the seal thickness is greatly different from 3 mm, relationships between steady infiltration rates and P_{125} will obviously vary).

Suctions across surface seals were measured for a number of soils under the laboratory rainfall simulator (Table 4), with good agreement between results from disc permeameters and gravimetric sampling for some soils only.

Table 4. Tensions across surface seals measured by either disc permeameters or by gravimetric sampling in laboratory and field studies

Soil ^A and tillage treatment ^B	Tension (mm water) across seals, as measured by:		
	Gravimetric sampling (Laboratory plots)	Laboratory plots	Disc permeameters on: Field plots
1. CT-S	48	50	ND
10.	60	60	50-65
11.	100	60	ND
16. DD+S	65	35-45	ND
17.	190	5-15	ND
19. CT+S	100	45-65	ND
20.	40	30-60	20-40
21.	205	30-60	10-20
22. DD+S	35	30	ND
RT+S	70	50-70	ND

^A Soils are numbered as in Table 1.

^B DD, direct drill; RT, reduced tillage; CT, conventional (frequent) tillage; S refers to crop residues (stubble) either retained during fallow (+) or removed (-).

^C ND, not determined.

For soils 17, 19 and 21, which have low steady infiltration rates and, hence, are likely to have low conductivities, there were large differences between suctions measured by gravimetric sampling and those measured by disc permeameters (Table 4). The failure of the disc permeameters to respond to the large suctions across the surface seals can be attributed to the extremely slow rate of water movement from the disc permeameter through the highly impermeable surface seals. Consequently, estimation of suction across seals using disc permeameters was successful only on the more stable and permeable soils.

Also, the slowness of the disc permeameters to respond to suctions across a seal led to concerns that water movement from the permeameter after 3-4 min was simply a response to drainage of the soil profile after rain had ceased.

Therefore, gravimetric sampling was adopted as the more useful method for assessing suctions across surface seals.

Suctions measured by gravimetric sampling (Table 4) were larger for lower seal conductivities, as suggested by Hillel and Gardner (1969). The actual suctions measured are similar to those reported by Sharma *et al.* (1981), giving confidence in the accuracy of the results. Suctions across surface seals and P_{125} in the surface seal under high energy rain were highly significantly related ($P < 0.001$) (Fig. 11).

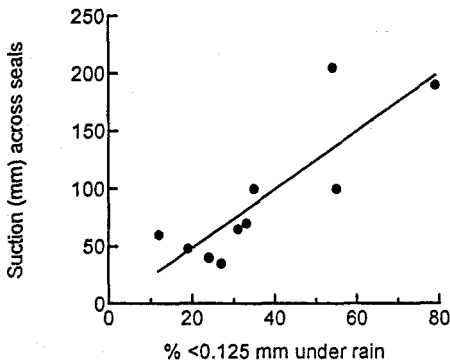


Fig. 11. Relationship between the suction (mm) across surface seals under high energy rain and P_{125} in the surface, $Y = 2.534X - 2.21$, $R^2 = 0.72$.

The relationship between P_{125} and suctions measured across the seals was then used to derive suctions across seals for all the soils studied under high energy rain, so that equation (4) could be used to calculate hydraulic conductivities of surface seals for all the soils for which infiltration under high energy rain was measured (Fig. 12).

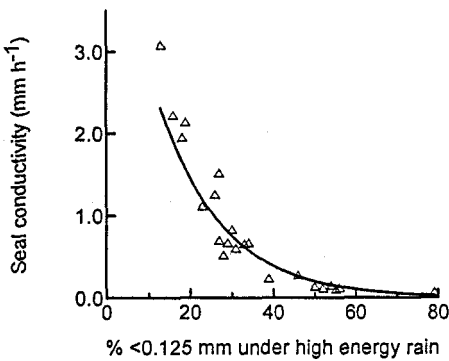


Fig. 12. Relationship between P_{125} in the surface and surface seal hydraulic conductivity, for soils under high energy rain, $Y = 5.429 e^{-0.0657X}$, $R^2 = 0.91$.

Conductivities of surface seals show a highly significant exponential relationship ($P < 0.001$) with P_{125} similar to that obtained for steady infiltration rates (Fig. 6a), in that the relationship appears to be strongest for higher proportions $<125 \mu\text{m}$. The higher suctions at higher proportions $<125 \mu\text{m}$ did not prevent flattening of the curve in that range.

Conclusions

The new method proposed for measuring size distributions at the soil surface under rain is remarkably successful in predicting the hydraulic behaviour of a

wide range of soils; far more successful than the more commonly used methods of measuring stability to wetting, especially for swelling soils. Therefore, if a test of aggregate stability/breakdown is intended to give information on the likely performance of a wide range of dryland soils under field conditions, wetting by rainfall (whether simulated or natural) is essential. It appears that wetting rates and, hence, intensities are of greater importance than rainfall kinetic energy in affecting breakdown on wetting, to the extent that accurate simulation of rainfall energy may not be crucial for studies of breakdown on wetting.

There is some flexibility in the size fractions that could be adopted as a measure of breakdown. Although there are theoretical reasons for using P_{125} , the size classes <250 and $<500 \mu\text{m}$ are also strongly correlated with soil hydraulic properties and could be used if changes in these larger size fractions were of particular interest. However, indices of aggregation such as MWD or GMD do not give an indication of the proportion of fine particles in the surface, and are not recommended. Measurements of particles $<125 \mu\text{m}$ could be used either as indicators of steady infiltration rates under certain conditions, or to estimate conductivities of surface seals developed under rainfall for modelling infiltration and runoff.

Relationships between proportions of fine material at the soil surface and steady infiltration rates showed that raindrop impact causes surface sealing and reduced infiltration by compacting the surface layer, rather than by increasing aggregate breakdown, as generally supposed. Therefore, accurate simulation of rainfall energy is important for studies of infiltration. Compaction of the surface and reduction of infiltration rates due to drop impacts occurs for even the most stable soils.

Acknowledgments

We are grateful to many of our colleagues in the Queensland Department of Primary Industries for assistance with rainfall simulator studies and/or access to data, including Mr S. Glanville, Mr E. Thomas, Mr D. Orange, Dr R. Chisholm, Dr B. Prove, Mrs J. Cleary, Mr G. G. Smith, and Mr D. M. Silburn. We thank Dr B. J. Bridge of CSIRO Division of Soils for his advice and assistance with measurements of infiltration into soil 23, and Mr B. Murphy of the New South Wales Soil Conservation Service for providing samples and infiltration data for soil 22. We thank the Wheat Research Council of Australia for funding the work of Mrs Cleary and Mr Smith.

References

- Al-Durrah, M. M., and Bradford, J. M. (1982). Parameters for describing soil detachment due to waterdrop impact. *Soil Sci. Soc. Am. J.* **46**, 836-40.
- Boon, W., and Savat, J. (1980). A nomogram for the prediction of rill erosion. In 'Soil Conservation. Problems and Prospects'. (Ed. R. P. C. Morgan.) pp. 303-19. (John Wiley: New York.)
- Bradford, J. M., Ferris, J. E., and Remley, P. A. (1987a). Interrill erosion processes. I. Effect of surface sealing on infiltration, runoff, and soil splash detachment. *Soil Sci. Soc. Am. J.* **51**, 1566-71.
- Bradford, J. M., Ferris, J. E., and Remley, P. A. (1987b). Interrill erosion processes. II. Relationships of splash detachment to soil properties. *Soil Sci. Soc. Am. J.* **51**, 1571-75.
- Brewer, R., and Blackmore, A. V. (1956). The effects of entrapped air and optically oriented clay on aggregate breakdown and soil consistence. *Aust. J. Appl. Sci.* **7**, 59-68.

- Bubenzer, G. D., and Meyer, L. D. (1965). Simulation of rainfall and soils for laboratory research. *Trans. ASAE* **8**, 73, 75.
- Carman, P. C. (1956). 'Flow of Gases through Porous Media'. (Butterworths: London.)
- Chaney, K., and Swift, R. S. (1984). The influence of organic matter on aggregate stability in some British soils. *J. Soil Sci.* **35**, 223-30.
- Cleary, J. L., Loch, R. J., and Thomas, E. C. (1987). Effects of time under rain, sampling technique and transport of samples on size distributions of water-stable aggregates. *Earth Surf. Proc. Landforms* **12**, 311-18.
- Connolly, R. D., Silburn, D. M., Ciesiolka, C. A. A., and Foley, J.L. (1991). Modelling hydrology of agricultural catchments using parameters derived from rainfall simulator data. *Soil Till. Res.* **20**, 33-44.
- Coughlan, K. J. (1979). Influence of microstructure on the physical properties of cracking clay soils. Report to the Reserve Bank, August, 1979.
- Coughlan, K. J. (1984). The structure of vertisols. In 'The Properties and Utilization of Cracking Clay Soils'. (Eds McGarity, Hoults and So.) Reviews in Rural Science No. 5, pp. 87-96. (Univ. of New England: Armidale, NSW.)
- Cruse, R. M., and Larson, W. E. (1977). Effect of soil shear strength on soil detachment due to raindrop impact. *Soil Sci. Soc. Am. J.* **41**, 777-81.
- Duley, F. L. (1939). Surface factors affecting the rate of intake of water by soils. *Soil Sci. Soc. Am. Proc.* **4**, 60-4.
- Duncan, M. J. (1972). The performance of a rainfall simulator and an investigation of plot hydrology. M.Agr.Sc. Thesis, Lincoln College, Univ. Canterbury, New Zealand.
- Epstein, E., and Grant, W. J. (1973). Soil crust formation as affected by raindrop impact. In 'Ecological Studies. IV. Physical Aspects of Soil Water and Salts in Ecosystems'. pp. 195-201. (Springer: Berlin.)
- Hillel, D., and Gardner, W. R. (1969). Steady infiltration into crust-topped profiles. *Soil Sci.* **108**, 137-42.
- Horn, M. E. (1971). Estimating soil permeability rates. *J. Irrig. Drainage Div. ASCE* **97** (IR2), 263-74.
- Joss, V. J., and Waldvogel, A. (1967). Ein spectrograph fur niederschlagestropher mit automatischer auswertung. *Pure Appl. Geophys.* **68**, 240-6.
- Loch, R. J. (1989). Aggregate breakdown under rain: its measurement and interpretation. Ph.D. Thesis, University of New England, Armidale.
- Loch, R. J. (1994). A method for measuring aggregate water stability with direct relevance to surface seal development under rainfall. *Aust. J. Soil Res.* **32**, 687-99.
- Loch, R. J., Cleary, J. L., Thomas, E. C., and Glanville, S. F. (1988). An evaluation of the use of size distributions of sediment in runoff as a measure of aggregate breakdown in the surface of a cracking clay soil under rain. *Earth Surf. Proc. Landforms* **13**, 37-44.
- McIntyre, D. S. (1958). Permeability measurements of soil crusts formed by raindrop impact. *Soil Sci.* **85**, 185-9.
- Marston, D. (1980). Rainfall simulation for the assessment of the effects of crop management on soil erosion. M. Nat. Res. Thesis, Univ. of New England, Armidale.
- Mason, D. D., Lutz, J. F., and Petersen, R. G. (1957). Hydraulic conductivity as related to certain soil properties in a number of Great Soil Groups—sampling errors involved. *Soil Sci. Soc. Am. Proc.* **21**, 554-60.
- Mazurak, A.P. (1949). Effect of gaseous phase on water-stable synthetic aggregates. *Soil Sci.* **69**, 135-48.
- Meyer, L. D., and McCune, D. L. (1958). Rainfall simulator for runoff plots. *Agric. Eng.* **39**, 644-8.
- Morin, J., Goldberg, D., and Seginer, I. (1967). A rainfall simulator with a rotating disc. *Trans. ASAE* **10**, 74-7, 79.
- Nearing, M. A., and West, L. T. (1988). Soil strength indices as indicators of consolidation. *Trans. ASAE* **31**, 471-6.
- Norton, L. D. (1987). Micromorphological study of surface seals developed under simulated rainfall. *Geoderma* **40**, 127-40.
- Perroux, K. M., and White, I. (1988). Designs for disc permeameters. *Soil Sci. Soc. Am. J.* **52**, 1205-15.

- Philip, J. R. (1957). The theory of infiltration. I. The infiltration equation and its solution. *Soil Sci.* **83**, 345–57.
- Schultz, J. P., Jarrett, A. R., and Hoover, J. R. (1985). Detachment and splash of a cohesive soil by rainfall. *Trans. ASAE* **28**, 1878–84.
- Sharma, P. P., Gantzer, C. J., and Blake, G. R. (1981). Hydraulic gradients across simulated rain-formed surface seals. *Soil Sci. Soc. Am. J.* **45**, 1031–34.
- Smith, G. D., Coughlan, K. J., and Fox, W. E. (1978). The role of texture in soil structure. In 'Modification of Soil Structure'. (Eds W. W. Emerson, R. D. Bond, and A. R. Dexter.) pp. 79–86. (John Wiley: New York.)
- Talsma, T. (1969). *In situ* measurement of sorptivity. *Aust. J. Soil Res.* **7**, 269–76.
- Williams, J., and Bonell, M. (1988). The influence of scale of measurement on the spatial and temporal variability of the Philip infiltration parameters—an experimental study in an Australian savannah woodland. *J. Hydrol.* **104**, 33–51.

Manuscript received 7 September 1993, accepted 22 February 1994